



## Molecular Crystals and Liquid Crystals Science and Technology. Section A. Molecular Crystals and Liquid Crystals

Publication details, including instructions for authors and  
subscription information:

<http://www.tandfonline.com/loi/gmcl19>

### Dielectric Study and Helical Pitch Measurements on a New Antiferroelectric Liquid Crystal

F. Bibonne<sup>a</sup>, J. P. Parneix<sup>a</sup>, N. Isaert<sup>b</sup>, G. Joly<sup>b</sup>, H. T. Nguyen<sup>c</sup>,  
A. Bouchta<sup>c</sup> & C. Destrade<sup>c</sup>

<sup>a</sup> Laboratoire de Physique des Interactions Ondes-Matières,  
E.N.S.C.P.B., U.R.A. CNRS 1506, 351 cours de la Liberation, 33405,  
TALENCE, FRANCE

<sup>b</sup> Laboratoire de Dynamique et Structure des Matériaux  
Moléculaires, Université de Lille 1, URA CNRS 801, 59655,  
VILLENEUVE, D'ASCO, FRANCE

<sup>c</sup> Centre de Recherche Paul Pascal, CNRS, Domaine Universitaire,  
Avenue du Docteur Schweitzer, 33600, PESSAC, FRANCE

Version of record first published: 23 Sep 2006.

To cite this article: F. Bibonne, J. P. Parneix, N. Isaert, G. Joly, H. T. Nguyen, A. Bouchta & C. Destrade (1995): Dielectric Study and Helical Pitch Measurements on a New Antiferroelectric Liquid Crystal, *Molecular Crystals and Liquid Crystals Science and Technology. Section A. Molecular Crystals and Liquid Crystals*, 263:1, 27-35

To link to this article: <http://dx.doi.org/10.1080/10587259508033567>

PLEASE SCROLL DOWN FOR ARTICLE

Full terms and conditions of use: <http://www.tandfonline.com/page/terms-and-conditions>

This article may be used for research, teaching, and private study purposes. Any substantial or systematic reproduction, redistribution, reselling, loan, sub-licensing, systematic supply, or distribution in any form to anyone is expressly forbidden.

The publisher does not give any warranty express or implied or make any representation that the contents will be complete or accurate or up to date. The accuracy of any instructions, formulae, and drug doses should be independently verified with primary sources. The publisher shall not be liable for any loss, actions, claims, proceedings,

demand, or costs or damages whatsoever or howsoever caused arising directly or indirectly in connection with or arising out of the use of this material.

## DIELECTRIC STUDY AND HELICAL PITCH MEASUREMENTS ON A NEW ANTIFERROELECTRIC LIQUID CRYSTAL

F. BIBONNE, J.P. PARNEIX

Laboratoire de Physique des Interactions Ondes-Matières, E.N.S.C.P.B., U.R.A.  
CNRS 1506, 351 cours de la Libération, 33405 TALENCE, FRANCE

N. ISAERT, G. JOLY

Laboratoire de Dynamique et Structure des Matériaux Moléculaires, Université de  
Lille 1, URA CNRS 801, 59655 VILLENEUVE D'ASCQ, FRANCE

H.T. NGUYEN, A. BOUCHTA, C. DESTRADE

Centre de Recherche Paul Pascal, CNRS, Domaine Universitaire, Avenue du  
Docteur Schweitzer, 33600 PESSAC, FRANCE

**Abstract** The dielectric dispersion in the ferroelectric and antiferroelectric phases of a new liquid crystal (S)-4-(1-methylheptyloxycarbonyl)-phenyl 4-(4-dodecyloxybenzoyloxy)benzoate has been investigated in the frequency range from 10 Hz to 10 MHz. The behaviour of the soft mode in SmA and the Goldstone mode in SmC\* have been determined. Two dielectric relaxations have been recognized in the antiferroelectric SmC<sub>A</sub>\* phase : the first one between 5 kHz and 50 kHz and the second one, also observable in the ferroelectric SmC<sub>FI</sub>\* phase, around 1 MHz. In SmC<sub>FI</sub>\*, a drastic change in the behaviour of the low frequency response has been found depending on whether the sample was heated or cooled. A sign reversal of the helical pitch has been determined inside the SmC<sub>FI</sub>\* phase, leading to low pitch values of opposite sign in SmC<sub>A</sub>\* and SmC\*.

## INTRODUCTION

Since the discovery of the antiferroelectric smectic phase (SmC<sub>A</sub>\*) as the origin of the tristable switching by Chandani *et al.*<sup>1,2</sup>, considerable attention has been paid to antiferroelectric liquid crystals (AFLC) because of their potential application to display devices.<sup>3</sup> The SmC<sub>A</sub>\* phase has a chiral smectic C structure with an antiferroelectric ordering : molecules in neighbouring layers are tilted from the layer normal in opposite directions, with a similar tilt angle. Hence, the dipole moments are cancelled out within two adjacent layers which implies the lack of a local spontaneous polarization.

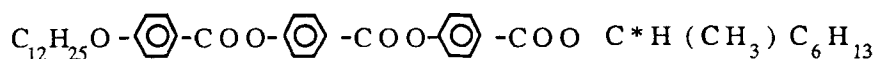
In addition to this SmC<sub>A</sub>\* phase, it has been pointed out that the chiral smectic C phase observed in some AFLCs can be divided into three subphases i.e. SmC<sub>α</sub>\*, SmC<sub>β</sub>\* (classical ferroelectric phase found in FLCs) and SmC<sub>γ</sub>\*.<sup>4</sup> The SmC<sub>α</sub>\* phase, appearing between the paraelectric SmA and the SmC<sub>β</sub>\* phases, usually exists only in a narrow

temperature interval. According to the switching characteristics<sup>5</sup>, the  $\text{SmC}_\alpha^*$  phase seems to show an antiferroelectric character just below the  $\text{SmA-SmC}_\alpha^*$  transition and becomes ferroelectric with decreasing temperature. The  $\text{SmC}_\gamma^*$  phase, intermediate between  $\text{SmC}_\beta^*$  and  $\text{SmC}_\alpha^*$ , was attributed to a ferroelectric phase by means of conoscopic observation<sup>6</sup> and D-E hysteresis behaviour<sup>7</sup>: several structures have been yet considered in order to describe this phase and a phenomenological model of antiferroelectric liquid crystals has been introduced.<sup>8,9,10</sup> Note that in the following we will designate the  $\text{SmC}_\beta^*$  and  $\text{SmC}_\gamma^*$  phases by  $\text{SmC}^*$  and  $\text{SmC}_{\text{FI}}^*$  respectively.

In this paper, we report the temperature dependence of dielectric dispersion, the relaxation behaviour and helical pitch measurements in a new AFLC exhibiting  $\text{SmC}_\alpha^*$  and  $\text{SmC}_{\text{FI}}^*$  phases.

## EXPERIMENTAL PROCEDURE

The sample used in this experiment was (S)-4-(1-methylheptyloxycarbonyl)-phenyl 4-(4-dodecyloxybenzoyloxy)benzoate,



which shows the following phase sequence :

Cryst-(69)- $\text{SmC}_\alpha^*$ -(98)- $\text{SmC}_{\text{FI}}^*$ -(99.3)- $\text{SmC}_{\text{FI}2}^*$ -(101)- $\text{SmC}^*$ -(121)- $\text{SmA}$ -(130)-Iso

The phase transition temperatures listed above were obtained by both microscopic observation and DSC but those in sandwich cells seriously depend on cell thickness.

Helical pitch measurements have been obtained with a polarizing microscope (Pamphot Leitz) equipped with a heating stage (Mettler FP52). The observed light is the reflected one. Basic experiments are performed on prismatic cells with weak angle according to the process already described.<sup>11</sup> For the compound studied, a good pseudo-homeotropic orientation is easily obtained in  $\text{SmC}^*$  phase, leading to the well-known Grandjean-Cano texture : many regular steps are observed that enable precise determination of the pitch and its dependance versus the temperature. So the compound is introduced in the cell during the  $\text{SmC}^*$  phase.

Dielectric measurements were performed with an impedance analyser (HP4192A) as detailed in a previous paper.<sup>12</sup> Sample cells were constructed from two glass substrates with patterned ITO, separated by 15  $\mu\text{m}$  thick spacers. The area of the electrodes was 9  $\text{mm}^2$ . Homogeneous alignment (planar orientation) was achieved by coating the glasses with polyimide and rubbing unidirectionally. An AC measuring field of 0.5 V was applied in a parallel direction to the smectic layers. After stabilizing the temperature, the real and imaginary parts  $\epsilon'$  and  $\epsilon''$  of the complex dielectric constant  $\epsilon^*$  ( $\epsilon^* = \epsilon' - j\epsilon''$ ) were carried out in the frequency range 10 Hz - 10 MHz during the cooling run as well as the heating run with the rate 0.1  $^\circ\text{C}/\text{min}$ . The alignment was optically controlled using a polarizing microscope with transmitted light.

## HELICAL PITCH MEASUREMENTS

In  $\text{SmC}^*$  phase, variation of the pitch value is weak on the most part of the existence domain :  $p = 0.36 \mu\text{m}$  at  $T = 104^\circ\text{C}$  down to  $p = 0.35 \mu\text{m}$  at  $T = 116.8^\circ\text{C}$ . When approaching the  $\text{SmA}$  phase strong damage of the texture appears but it is accompanied with a defiling of the visible reflected colors that enables pitch variations measurements: quick changes from green to purple colors correspond to the end of the half pitch reflexion ( $\lambda \cong np$ ) ; then appears the whole visible spectrum, from red to purple corresponding to the full pitch reflexion ( $\lambda \cong 2np$ ). There the pitch varies between  $p = 0.2 \mu\text{m}$  and  $p = 0.13 \mu\text{m}$  at  $T = 118^\circ\text{C}$  and  $T = 118.6^\circ\text{C}$ .

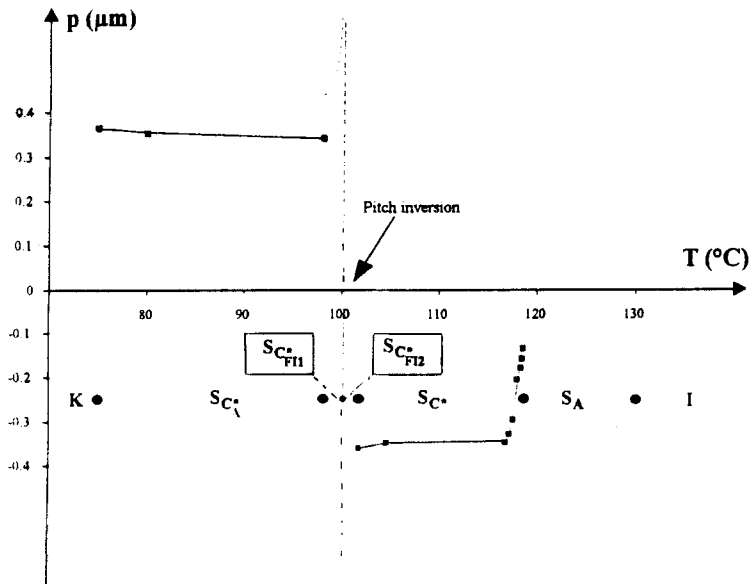


FIGURE 1 Helical pitch variation versus temperature

Rapid cooling ( $T = 2^\circ\text{C}/\text{min}$ ) leads to the  $\text{SmC}_A^*$  phase exhibiting small pitches deduced from the observation of the selective reflexion colors : clear green corresponding to  $p \cong 0.36 \mu\text{m}$  at  $T = 80^\circ\text{C}$ . Pitch variations are weak on the whole  $\text{SmC}_A^*$  as shown by Fig. 1. When the temperature increases, spectacular phenomena occur between  $\text{SmC}_A^*$  and  $\text{SmC}^*$  phases : the characteristic stable color of the  $\text{SmC}_A^*$  moves quickly towards the red one, showing the phase transition to a less strongly twisted - ferroelectric - phase. The colors that follow are situated on the red side of the visible spectrum : they are hardly detectable but their modification rate shows that the twist diminishes slower than during the  $\text{SmC}_A^* - \text{SmC}_{FI1}^*$  transition as suggested by dotted curves. Near the  $\text{SmC}^*$  phase, the succession of the above described phenomena occurs in opposite order, corresponding to the  $\text{SmC}_{FI2}^*$  phase and its transition to  $\text{SmC}^*$ .

The sign of pitches ( $> 0$  for a dextro-structure) have been determined in the following way : the selectively reflected light is extinguished with a circular analyser.

The well-known relation between the sense of selective reflexion and the twist of the structure leads to the required sign. For this compound the  $\text{SmC}_A^*$  phase is dextro-structure while the  $\text{SmC}^*$  phase is leavo-structure. For ferroelectric phases, the sign of twist is then deduced by continuity. As explained above, when increasing the temperature during the  $\text{SmC}_{\text{FI1}}^*$  and  $\text{SmC}_{\text{FI2}}^*$  phases is observed the disparition and the reappearance of optical visible colors : that observation accompanies the sign reversal of the pitch. This "Pitch inversion" is quoted on the figure ; it occurs at  $T = 100.6^\circ\text{C}$ . But it remains a question : is the pitch inversion temperature the signature of the transition between  $\text{SmC}_{\text{FI1}}^*$  and  $\text{SmC}_{\text{FI2}}^*$  phases ?

## DIELECTRIC MEASUREMENTS

Typical dispersion curves in each phase obtained during the cooling process, as well as the dielectric response in the  $\text{SmC}_{\text{FI}}^*$  phase in the heating process, are plotted in Fig. 2. Note that each coordinate is properly scaled and that results below 100 Hz are not shown because of a large experimental error in the measurement which is affected by conductivity at low frequencies. Several relaxation modes occur while decreasing temperature and manifest as maxima on the imaginary part of dispersion, corresponding to relaxation frequencies. First of all, the small peak appearing in  $\epsilon''$  curves at about 10 MHz is an artifact caused by the ITO layer resistance. In  $\text{SmA}$ , the relaxation at 500 kHz is due to the well-known soft mode described as the fluctuation of the molecular tilt angle. This mode also exists in  $\text{SmC}^*$  but we only observe the Goldstone mode at 5 kHz because of its a larger amplitude. The Goldstone mode is associated with the fluctuation of the azimuthal angle around the helical axis. Dielectric spectra do not allow us to distinguish the two ferroelectric phases  $\text{SmC}_{\text{FI1}}^*$  and  $\text{SmC}_{\text{FI2}}^*$  : when cooling from  $\text{SmC}^*$ , the  $\text{SmC}_{\text{FI}}^*$  phase has a dielectric relaxation around 5 kHz in his highest temperature range whereas a low frequency relaxation at 200 Hz is clearly distinguished in the heating process as illustrated by Fig. 2d. In  $\text{SmC}_A^*$ , we recognize a small amplitude relaxation at 40 kHz. At last, we find an high frequency relaxation mode, which is also a small amplitude one, in both  $\text{SmC}_{\text{FI}}^*$  and  $\text{SmC}_A^*$  phases : its frequency increases from 500 kHz in  $\text{SmC}_{\text{FI}}^*$  to 1 MHz in  $\text{SmC}_A^*$ .

In Fig. 3, we show the temperature dependence at cooling of the dielectric constant  $\epsilon'$  at several frequencies and the different relaxation frequencies. In  $\text{SmA}$ , the soft mode obeys to the Curie-Weiss law : on approaching the  $\text{SmC}^*$  phase, the relaxation frequency  $f_r$  decreases linearly with decreasing temperature. Note that we choose a logarithmic scale on frequency axis so that the linear behaviour is not revealed. At high frequencies, the temperature dependent part of  $\epsilon'$  around the  $\text{SmA-SmC}^*$  transition is only due to the soft mode and reaches its maximum at the transition. In  $\text{SmC}^*$ , the relaxation frequency is almost constant at 5 kHz except in a few degrees below the  $\text{SmA}$  phase where  $f_r$  and the contribution to  $\epsilon'$  exhibit a minimum and a maximum respectively. This result is connected with the behaviour of the helicoidal pitch  $p$  in  $\text{SmC}^*$  phase since  $f_r$  is expected to be proportional to  $(1/p^2)^{13,14}$  : as reported in Fig. 1, the pitch also reaches a maximum at  $2^\circ\text{C}$  below the transition from  $\text{SmA}$ . At

the  $\text{SmC}^* \text{-SmC}_{\text{FI}}^*$  transition,  $\epsilon'$  slightly increases at 100 kHz while it decreases at lower frequencies.

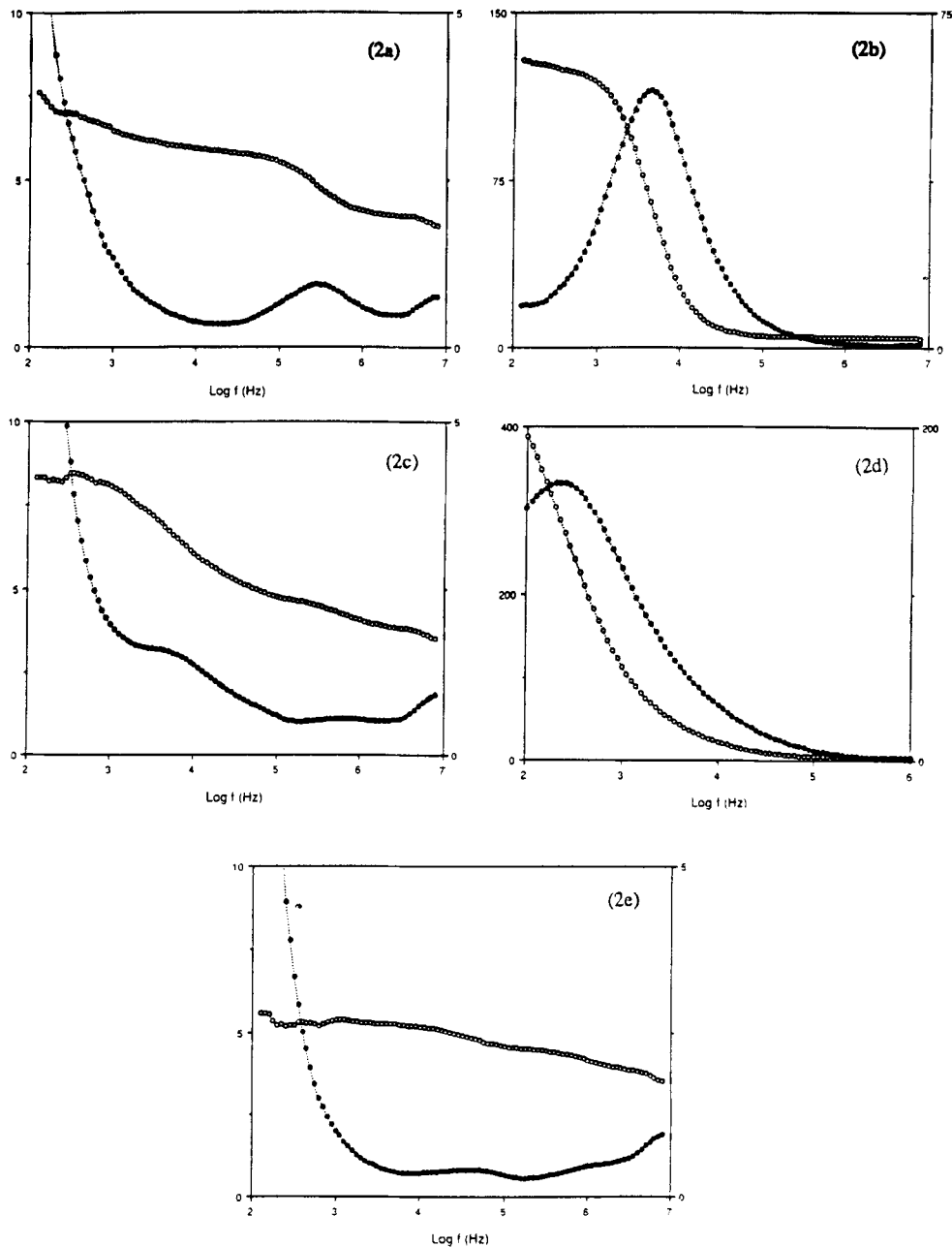


FIGURE 2 Typical dielectric dispersion curves in (a)  $\text{SmA}$  123 °C, (b)  $\text{SmC}^*$  119 °C, (c)  $\text{SmC}_{\text{FI}}^*$  at cooling 99.5 °C, (d)  $\text{SmC}_{\text{FI}}^*$  at heating 102 °C, (e)  $\text{SmC}_{\text{A}}^*$  95.5 °C  $\epsilon'$  open circles,  $\epsilon''$  closed circles

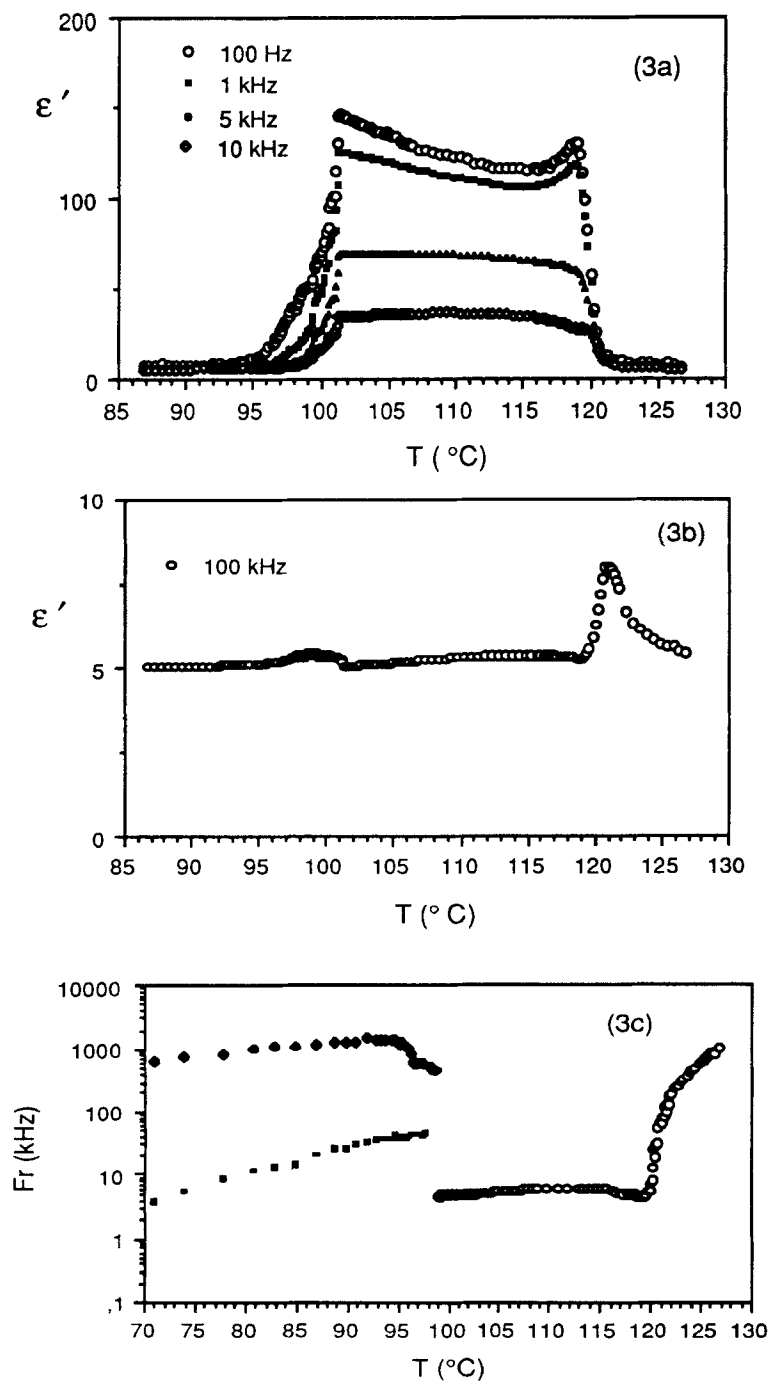


FIGURE 3 Temperature dependence at cooling of (a) the dielectric constant for 100 Hz, 1 kHz, 5 kHz, 10 kHz, (b) the dielectric constant for 100 kHz, (c) the relaxation frequency



In  $\text{SmC}_{\text{FI}}^*$ , two different dielectric spectra are obtained depending on cooling or heating the sample. Consequently, we also report in Fig. 4 the temperature dependence at heating of  $\epsilon'$  and the relaxation frequencies.

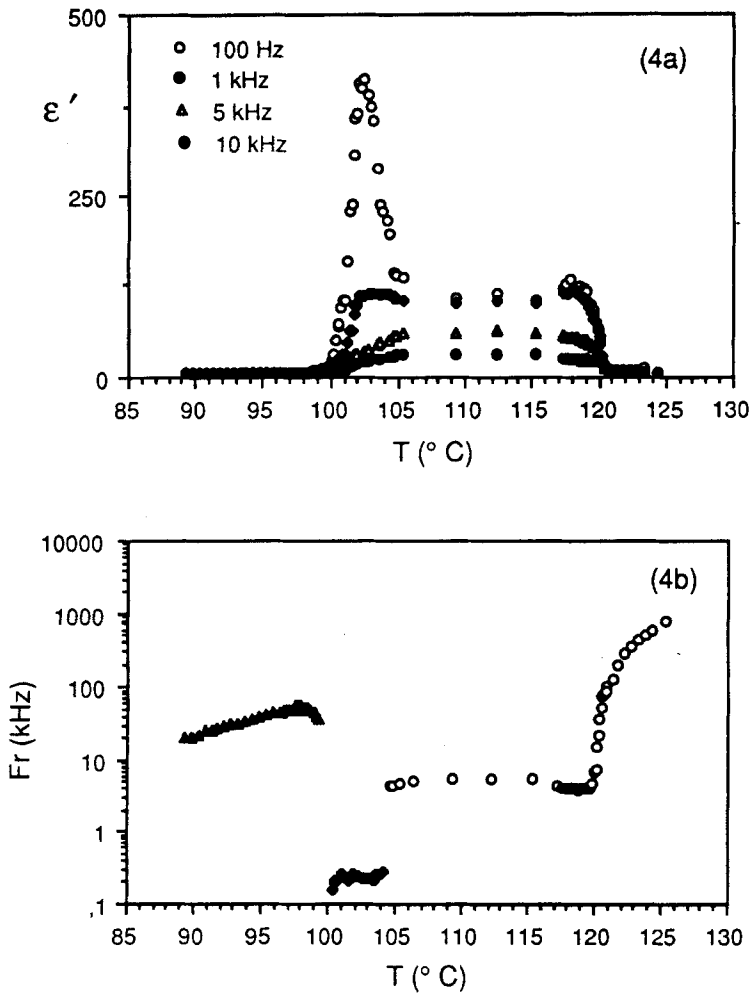


FIGURE 4 Temperature dependence at heating of (a) the dielectric constant for 100 Hz, 1 kHz, 5 kHz, 10 kHz, (b) the relaxation frequency

On the one hand, at cooling  $\epsilon'$  falls down to the value in the antiferroelectric phase but a relaxation in the same frequency range as the Goldstone mode in  $\text{SmC}^*$  still remains observable over 1.5  $^{\circ}\text{C}$ , and may be attributed to the Goldstone mode in  $\text{SmC}_{\text{FI}}^*$ : its strength is smaller than in  $\text{SmC}^*$  because of the partial compensation of the local dipole moments in the  $\text{SmC}_{\text{FI}}^*$  phase. Furthermore, an high frequency relaxation is found which frequency increases with decreasing temperature until it reaches 1.4 MHz in  $\text{SmC}_{\text{A}}^*$  and then slowly decreases. We may describe this relaxation process as the soft mode. On the

other hand, we observe in the heating process a large amplitude relaxation at about 200 Hz in a 4 °C temperature interval around the  $\text{SmC}_A^*-\text{SmC}_{FI}^*$  transition. In the same way, a peak occurs on  $\epsilon'$  curves at 100 Hz, which maximum is about 400 while the one at cooling is only 150. As recently proposed<sup>15,16</sup>, the  $\text{SmC}_{FI}^*$  phase could be considered as a bilayer structure with an almost constant tilt angle and a difference in the azimuthal angle of two adjacent layers which is neither 0° nor 180°. Then, an antiphase azimuthal mode is expected to have a low-frequency contribution, maximum at the  $\text{SmC}_A^*-\text{SmC}_{FI}^*$  transition. But the relation between this mode and our low-frequency relaxation, and the reason why the low frequency dielectric response is so different between cooling and heating are not clarified at this stage.

In  $\text{SmC}_A^*$ , apart from the soft mode already mentioned around 1 MHz, we recognize another small amplitude relaxation. Fr increases linearly from 5 kHz to 50 kHz with increasing temperature and can be characterized by an activation energy of 0.45 eV. Some authors have reported that this relaxation mode appears for both homogeneously and homeotropically aligned cells in an other AFLC<sup>17</sup>. It leads us to attribute this mode to the rotation around the short axis of molecules<sup>18</sup>.

In summary, dielectric properties have been investigated as functions of frequency and temperature for the compound n=12 of a new series of antiferroelectric liquid crystals. In addition to the soft mode and the Goldstone mode in  $\text{SmA}$  and  $\text{SmC}^*$  respectively, we have found others dielectric relaxations : in  $\text{SmC}_A^*$ , two modes which may be connected with a rotation around the short axis of molecules and a soft mode; in  $\text{SmC}_{FI}^*$ , the Goldstone mode just below  $\text{SmC}^*$  and the soft mode but also a low frequency mode which origin is still to be determined.

We now intend to study all the compounds of the series, some of them with short alkoxy chain displaying the  $\text{SmC}_\alpha^*$  phase, and also the effect of a DC Bias field on the dielectric strength and the relaxation frequency, which may add further information to the vibrational modes and the structures of these phases.

## REFERENCES

1. A. D. L. Chandani, Y. Ouchi, H. Takezoe, A. Fukuda, K. Terashima, K. Furukawa and A. Kishi, *Jpn. J. Appl. Phys.*, **28** (7), L1261, (1989)
2. A. D. L. Chandani, E. Gorecka, Y. Ouchi, H. Takezoe and A. Fukuda, *Jpn. J. Appl. Phys.*, **28** (7), L1265, (1989)
3. H. Orihara and Y. Ishibashi, *Ferroelectrics*, **122**, 177, (1991)
4. K. Hiraoka, A. Taguchi, Y. Ouchi, H. Takezoe and A. Fukuda, *Jpn. J. Appl. Phys.*, **29** (1), L103, (1990)
5. Y. Takanishi, K. Hiraoka, V. K. Agrawal, H. Takezoe, A. Fukuda and M. Matsushita, *Jpn. J. Appl. Phys.*, **30** (9A), 2023, (1990)
6. E. Gorecka, A. D. L. Chandani, Y. Ouchi, H. Takezoe and A. Fukuda, *Jpn. J. Appl. Phys.*, **29** (1), 131, (1990)

7. J. Lee, A. D. L. Chandani, K. Itoh, H. Takezoe and A. Fukuda, Jpn. J. Appl. Phys., **29** (6), 1122, (1990)
8. H. Orihara and Y. Ishibashi, Jpn. J. Appl. Phys., **29** (1), L115, (1990)
9. B. Zeks, R. Blinc and M. Cepic, Ferroelectrics, **122**, 221, (1991)
10. B. Zeks and M. Cepic, Liq. Cryst., **14** (2), 445, (1993)
11. M. Brunet and N. Isaert, Ferroelectrics, **84**, 25, (1988)
12. C. Legrand and J. P. Parneix, J. Phys. France, **51**, 787, (1990)
13. P. Martinot-Lagarde and G. Durand, J. Phys. Paris, **42**, 269, (1981)
14. T. Carlsson, B. Zeks, C. Filipic, A. Levstik and R. Blinc, Mol. Cryst. Liq. Cryst., **163**, 11, (1988)
15. V. L. Lorman, A. A. Bulbitch and P. Toledano, Phys. Rev. E, **49**, 2, (1994)
16. P. Gisse, J. Pavel, H. T. Nguyen and V. L. Lorman, to be published in Ferroelectrics
17. H. Moritake, M. Ozaki and K. Yoshino, Jpn. J. Appl. Phys., **32** (10A), L1432, (1993)
18. L. Benguigui, J. Phys., **43**, 915, (1982)